Formation of Molecularly Ordered Layered Mesoporous Silica via Phase Transformation of Silicate−Surfactant Composites

Yongde Xia, Robert Mokaya,* and Jeremy J. Titman

School of Chemistry, University of Nottingham, University Park, Nottingham NG7 2RD, U.K.

Received: January 14, 2004; In Final Form: May 21, 2004

We have prepared molecularly ordered layered silicate−surfactant mesophases from the stepwise phase transformation of surfactant−silicate composites. The hexagonal−cubic−lamellar phase transformations were achieved by varying the time allowed for hydrothermal crystallization of simple $CTAOH/SiO_2/H_2O$ systems at 135 °C. At short (3 h) crystallization periods, the hexagonal phase (MCM-41) was obtained, which after 24 h transformed into a cubic (MCM-48) phase stable for up to 4 days. At 6 days a mixture of cubic and lamellar phases was observed, which finally transformed into the molecularly ordered pure lamellar phase after 12 days of hydrothermal synthesis. Molecular ordering, which was probed using powder XRD and silicon-29 solid state NMR, was only observed for the lamellar phase. Crystallization of the silica framework, at long hydrothermal synthesis time, therefore acts as a driving force for the high to low curvature cubic−lamellar transformation. The phase transformations were accompanied by changes in particle morphology and gradual densification of the silica network. The molecular ordering of the layered material was, to some extent, retained after template removal by calcination. The calcined molecularly ordered layered mesoporous silica exhibited structurally well-ordered domains and had relatively high surface area and pore volume.

1. Introduction

The design and synthesis of materials that have a well-defined pore structure and framework, similar to that of zeolites, but with larger pores has been a main research goal in materials research over the past decade. The recent synthesis of the M41S family of mesoporous solids[1,2] has to some extent achieved this goal. The M41S family of mesoporous silicas, which possess well-ordered pores of diameter in the range 20−100 Å, have given rise to the hope of preparing materials that carry over the stability and well-defined structure of zeolites into the mesoporous range. However, M41S mesoporous silicas differ from crystalline zeolites in the nature of ordering in their pore walls. The pore walls of crystalline zeolites are ordered at the atomic level while for M41S mesoporous silicas the pore walls are amorphous. Therefore, despite their excellent structural ordering and well-defined pore size distribution, mesoporous silicas possess a largely amorphous inorganic framework, which in many ways exhibits properties similar to those of disordered amorphous silica.[2] The preparation of mesoporous silicas, which possess molecular ordering comparable to that of zeolites, is therefore desirable. The formation of zeotype mesoporous silicas is elusive because, in general, supramolecular templating (with longer chain surfactant molecules) and low to medium (typically <160 °C) temperatures are used in the preparation of mesoporous materials while microporous (zeolite) materials are synthesized via molecular templating (with shorter chain molecules as templates) at high (>150 °C) temperatures.

In an effort to impart zeolitic characteristics into mesoporous materials, composite zeolite/mesoporous silica materials have been prepared.[3−11] The composite materials are basically mixtures of the two components with varying degrees of integration. Typically, the zeolite/mesoporous composites are prepared through a two-step crystallization process in which a colloidal gel of lowly crystallized zeolite precursor is first prepared and then added to a solution of suitable surfactant molecules.[3−5] Dual templating with both long surfactant molecules and small chain amines has also been used in an effort to prepare mesoporous materials with zeolite frameworks.[6] Zeolites have also been used as a source of silica and alumina in the preparation of zeolite/mesoporous molecular sieve composites.[7] The concept of zeolite/mesoporous composite materials has been extended to include transformation[8−10] or coating[11] of the amorphous walls of a mesoporous aluminosilicate into a semicrystalline pseudo-zeolitic framework. Partial recrystallization of the interporous surface of mesoporous aluminosilicates can generate mesoporous/zeolite composites[9,10] or materials with surface-tectosilicate units.[8] The assembly of aluminosilicate mesostructures from preformed nanoclustered zeolite (Y, ZSM-5 or beta) seeds has been used as a route to zeolitization of mesoporous aluminosilicates.[12−14]

To date, very few studies have reported the preparation of mesoporous silica mesophases with molecular ordering within the pore walls. Christiansen et al.[15] reported the formation of molecularly ordered layered silicate−surfactant mesophases obtained by systematically varying the charge density and symmetry of the surfactant headgroup moieties. The extent of molecular ordering within the silicate framework was reported to be generally higher at longer (hydrothermal) crystallization times.[15] Wang and Exarhos[16] carried out a study of the local molecular ordering of such layered surfactant−silicate composites and identified temperature and gel composition as factors that influence local molecular ordering. The synthesis gels and conditions used in these previous studies[15,16] favored the direct formation of the layered silica. We, on the other hand, have reported that increase in the time allowed for hydrothermal crystallization during high-temperature (150 °C) synthesis of mesoporous silica MCM-41 can result in some ordering

* To whom correspondence should be addressed. E-mail: r.mokaya@nottingham.ac.uk.

10.1021/jp049813q CCC: $27.50
Published on Web 07/01/2004

(nanocrystallites) within the pore walls.[17] The pure silica MCM-41 materials with pore wall ordering (nanocrystallites) were obtained by extending the time allowed for hydrothermal crystallization in an otherwise normal MCM-41 synthesis procedure.[17] The time allowed for crystallization is therefore an important factor in the preparation of mesoporous silicas with semicrystalline or crystalline pore walls[15,17] and deserves further investigation.

Several recent studies have reported on the restructuring of surfactant−silicate mesophases during extended hydrothermal treatment. For example, Landry et al.,[18] Tolbert et al.,[19] and Gross et al.[20] have studied the phase transformation of mesoporous silica−surfactant composites under hydrothermal conditions. Landry et al. found that, during extended hydrothermal treatment, hexagonal (MCM-41) to cubic (MCM-48) phase transformation can occur.[18] The phase transformations proceeded in an epitaxial manner without dissolution of the original MCM-41 phase.[18] Romero et al.[21] observed a hexagonal to cubic to lamellar phase transformation using TEOS as a silica source and a mixture of CTAOH/CTABr as surfactant in a synthesis regime that included the gradual release of ethanol (formed from hydrolysis of the TEOS) and water from the synthesis gel during the hydrothermal crystallization. Xu and co-workers,[22] on the other hand, observed the formation of layered mesoporous silica phase from the sequential transformation of a disordered tubular phase to a lamellar phase which transformed to cubic (MCM-48) phase and finally to a second layered phase.

We have recently shown that highly ordered cubic crystals of MCM-48 mesoporous silica may be prepared from simple $CTAOH/SiO_2/H_2O$ systems under hydrothermal conditions.[23] We have now investigated the influence of changing the time allowed for hydrothermal crystallization under otherwise similar experimental conditions.[23] Here, we describe phase transformations from hexagonal (MCM-41) to cubic (MCM-48) and finally to a molecularly ordered lamellar mesostructure achieved by simply changing the time allowed for hydrothermal crystallization. The transformation from the cubic to lamellar phase is accompanied by the emergence of molecular ordering in the silica pore walls. This differs from previous reports where the molecularly ordered lamellar silicate−surfactant composites were prepared directly.[15,16] Our findings therefore shed some light on the mechanisms via which the formation of molecularly ordered mesoporous silica mesophases occurs. We also report, for the first time, characterization of calcined molecularly ordered lamellar silica and show that it is possible to obtain a (meso) porous material that, to some extent, retains some molecular and structural ordering after template removal by calcination.

2. Materials and Methods

2.1. Materials. The mesoporous silica materials were prepared as previously described,[23] except that the time allowed for hydrothermal crystallization was varied between 3 h and 12 days. In a typical synthesis, 2.14 g of fumed silica (Sigma) was added to 30 g of 10% cetyltrimethylammonium hydroxide (CTAOH) solution (Aldrich) under stirring to give a gel mixture of molar ratio 1:0.28:42 SiO_2:CTAOH:H_2O. After continuous stirring for 2 h at room temperature, the resulting gel was transferred to a Teflon-lined autoclave and heated at 135 °C for periods of time varying between 3 h and 12 days. At the expiry of the hydrothermal synthesis (or crystallization) period, the autoclave was cooled to room temperature and the solid product obtained by filtration followed by repeated washing with a large amount of distilled water. Five samples were prepared from crystallization periods of 3 h, 1 day, 4 days, 6 days, and 12 days. After drying in air at room temperature, the dry (as-synthesized) silicate−surfactant mesophases were calcined in air at 550 °C for 6 h to yield the mesoporous silicas.

2.2. Characterization. Powder XRD analysis was performed using a Philips PW1830 diffractometer with Cu Kα radiation (40 KV, 40 mA), 0.02° step size, and 1-s step time. Nitrogen sorption isotherms and textural properties of the materials were determined at −196 °C using nitrogen in a conventional volumetric technique by a Coulter SA3100 sorptometer. Before analysis the samples were oven-dried at 150 °C and evacuated for 12 h at 200 °C under vacuum. The surface area was calculated using the BET method based on adsorption data in the partial pressure (P/P_0) range 0.05−0.2 and total pore volume was determined from the amount of the nitrogen adsorbed at P/P_0 = ca. 0.99. ^{29}Si magic angle spinning (MAS) nuclear magnetic resonance (NMR) spectra were acquired from a cross-polarization MAS experiment with silicon-29 Larmor frequency of 59.61 MHz, acquisition time of 20 ms, total spectral width of 50 kHz, relaxation delay of 1 s, contact time of 4 ms, proton B1 field strength of 68 kHz, and a MAS rate of 2.3 kHz. The MAS rate was sufficient to ensure that spinning sidebands were outside the range of the isotropic shifts. The Hartman Hahn match was found using kaolinite and the spectrum was referenced externally to tetramethylsilane (TMS). Thermogravimetric analysis (TGA) was performed using a Perkin-Elmer TGA 6 analyzer with a heating rate of 20 °C/min under nitrogen flow of 25 mL/min. Transmission electron microscopy (TEM) images were recorded on a JEOL 2000-FX electron microscope operating at 200 kV. Samples for analysis were prepared by spreading them on a holey carbon film supported on a grid. Scanning electron microscopy (SEM) images were recorded using a JEOL JSM-820 scanning electron microscope. Samples were mounted using a conductive carbon double-sided sticky tape. A thin (ca. 10 nm) coating of gold sputter was deposited onto the samples to reduce the effects of charging.

3. Results and Discussion

3.1. Changes in Structural Ordering, Porosity, and Morphology Induced by Phase Transformations. Powder X-ray diffraction (XRD) may be used to distinguish various mesoporous silica phases.[1] The powder XRD patterns for the as-synthesized (silicate−surfactant mesophases) and calcined mesoporous silicas, obtained from crystallization periods between 3 h and 12 days are shown in Figure 1. The pattern of the material obtained after a crystallization period of 3 h is typical of a relatively well-ordered MCM-41; the as-synthesized sample shows an intense (100) diffraction peak and three higher order (110), (200), and (210) peaks, indicating good long-range ordering.[2] The calcined sample is less well-ordered and exhibits only one higher order peak. Calcination also induces a contraction (ca. 11%) of the basal spacing and lattice as shown in Table 1. This indicates that the MCM-41 material obtained after 3-h synthesis is relatively unstable to calcination. However, it is very clear from the XRD patterns that hydrothermal synthesis for 3 h results in a hexagonal (*p*6*m*) phase MCM-41 mesoporous silica.[1,2] The XRD patterns of the materials obtained after crystallization between 1 and 4 days are typical of highly ordered MCM-48 materials (indexed in a cubic mesophase of space group *Ia*3*d*) and show an intense (211) diffraction peak and several well-resolved higher order peaks.[23,24] Calcination of these MCM-48 materials induced small lattice contraction (8.5 and 1.4% for the 1- and 4-day samples, respectively) but with no significant effect on structural ordering. These materials (1 and

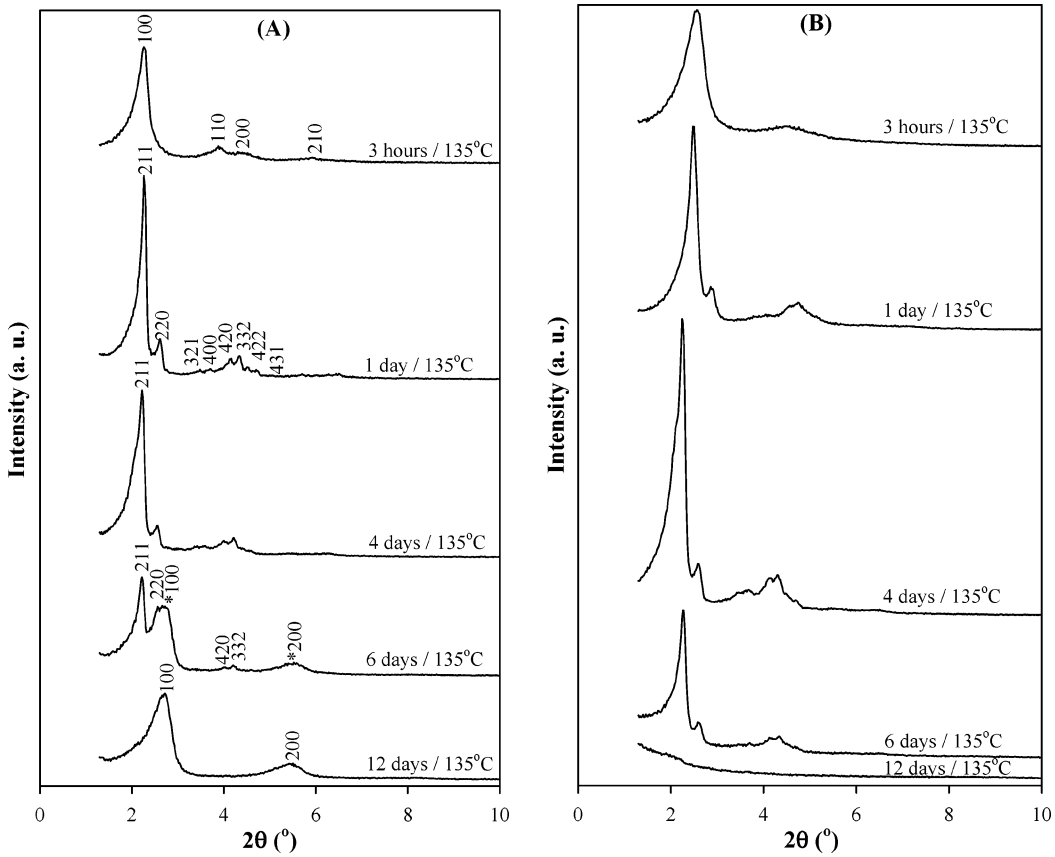

Figure 1. Powder XRD patterns of as-synthesized silicate−surfactant mesophases (A) and calcined mesoporous silicas (B) obtained from the hydrothermal crystallization of synthesis gels (of molar composition 1:0.28:42 SiO_2:CTAOH:H_2O) at 135 °C for various periods of time.

TABLE 1: Textural Properties of Mesoporous Silica Materials Synthesized from Hydrothermal Crystallization of CTAOH/SiO_2/H_2O Systems at 135 °C for Various Periods of Time

synthesis conditions[a]	mesoporous phase	basal spacing[b] (Å)	lattice parameter a_o[b,c] (Å)	surface area (m^2/g)	pore volume[d] (cm^3/g)	pore size[e] (Å)
135 °C/3 h	hexagonal	34.5 (38.9)	39.8 (44.9)	1403	1.07	37.3
135 °C/1 d	cubic	35.4 (38.7)	86.7 (94.8)	1247	1.10 (1.01)	34.1
135 °C/4 d	cubic	39.3 (39.9)	96.3 (97.7)	1140	1.13 (1.10)	38.6
135 °C/6 d	cubic/lamellar	39.0 (40.2)[f]	95.5 (98.5)[f]	757	0.78 (0.68)	36.0
135 °C/12 d	lamellar[g]	− (33.1)	−	637	0.68 (0.63)	

[a] h = hours and d = days. [b] Values in parentheses are for as-synthesized samples. [c] The lattice parameter a_o was obtained using the formula $a_o = 2d_{100}/\sqrt{3}$ or $a_0 = d_{211}\sqrt{6}$ for hexagonal and cubic phases, respectively. [d] Values in parentheses are mesopore volume. [e] Pore size obtained from the formula, pore size $= 4V_{meso}/S$, where V_{meso} is the mesopore volume and S is the surface area. [f] Values for cubic phase only. [g] Molecularly ordered lamellar phase.

4 days) are pure cubic phase and exhibit no XRD peaks above 10° 2θ (see Figure 1 in the Supporting Information), indicating the absence of molecular ordering. The XRD pattern of the as-synthesized sample crystallized for 6 days shows several peaks that cannot all be ascribed to any one pure phase material and in addition shows peaks above 10° 2θ, indicative of molecular ordering in the silica network (see Figure 1 in the Supporting Information).[15,16] For the as-synthesized sample synthesized for 6 days, we have assigned the "new" peaks observed below 10° 2θ (as shown in Figure 1A) as (100) and (200) peaks of a new layered silica phase. In assigning peaks for the 6-days synthesized sample, we have considered the fact that the d spacing ratio between the peaks assigned as (211) and (220) peaks is 0.866, which is consistent with cubic MCM-48 phase (space group $Ia3d$). For the new peaks, the d spacing ratio between peak (100) and peak (200) is 0.496, consistent with a lamellar phase for which the ratio is typically 0.5. The sample synthesized for 6 days is therefore a mixture containing cubic and lamellar silicate−surfactant phases.[25] On calcination, the lamellar phase collapses and all peaks associated with it are not observed. The calcined sample only shows evidence of cubic MCM-48 phase.

The XRD pattern of the sample crystallized for 12 days, which exhibits (100) and (200) peaks and other peaks at 2θ values above 10°, is consistent with the formation of a well-ordered pure phase lamellar material with nanoscale or molecular ordering within the pore walls.[15,16] On calcination, the lamellar (h00) peaks are largely lost due to the apparent loss of lamellar structural ordering. However, there is evidence of a residual peak (shoulder) at low 2θ values (perhaps 100 peak). Furthermore, the peaks, at 2θ values above 10°, assigned to molecular ordering within the silica framework[15,16] are still observed even after calcination as shown in Figure 2. The XRD patterns observed here for the as-synthesized sample crystallized for 12 days are similar to those previously reported for molecularly ordered layered silicate−surfactant composites.[15,16] In previous studies, which only investigated as-synthesized materials,[15,16,26] the two broad peaks at high 2θ values were attributed to ordering of surfactant molecules strongly interacting

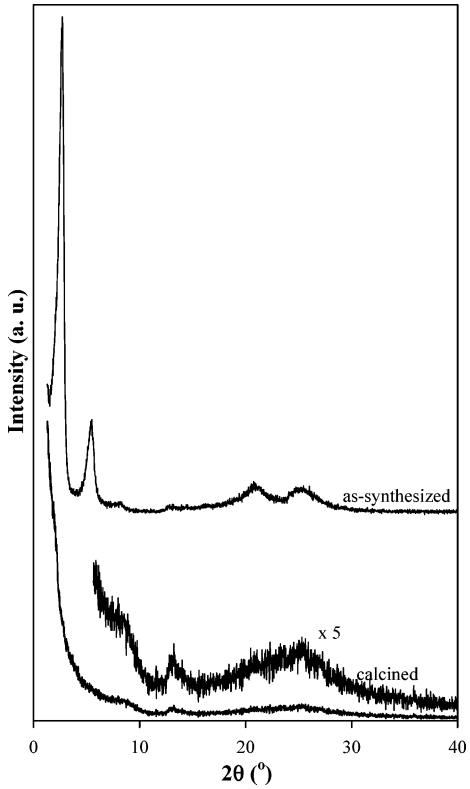

Figure 2. Powder XRD patterns of molecularly ordered layered silicate−surfactant mesophase obtained after hydrothermal synthesis 12 days, before, and after calcination.

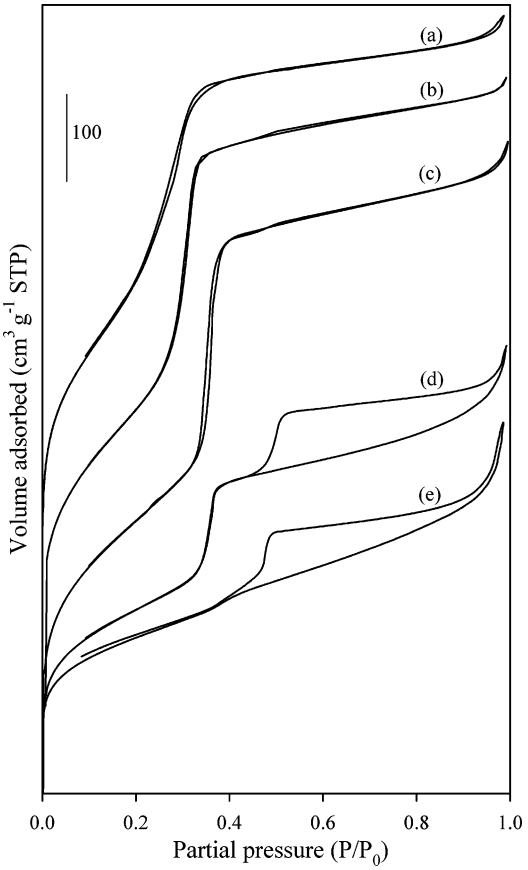

Figure 3. Nitrogen sorption isotherms of calcined mesoporous silicas obtained from the hydrothermal crystallization of synthesis gels (of molar composition 1:0.28:42 SiO_2:CTAOH:H_2O) at 135 °C for (a) 3 h, (b) 1 day, (c) 4 days, (d) 6 days, and (e) 12 days. For clarity isotherms a and b are offset on the *y* axis.

with the silica within the silicate−surfactant mesophase. Figure 2 shows that these peaks are present for calcined surfactant-free silica, thereby suggesting that they may also be a characteristic of molecular ordering within the silica network.

The nitrogen sorption isotherms for all the calcined materials are shown in Figure 3 and Table 1 gives their textural properties. The pure phase, hexagonal (3 h) and cubic (1 and 4 days), samples exhibit sorption isotherms with a well-developed step in the relative pressure (P/P_o) range 0.25−0.45 characteristic of capillary condensation (filling) into uniform mesopores. The isotherms therefore indicate that these samples are structurally well-ordered with a narrow pore size distribution, which is consistent with their XRD patterns (Figure 1) and high surface area and pore volume (Table 1). The pure phase cubic (MCM-48) materials obtained after crystallization for 1 or 4 days are particularly well-ordered.[23,24] The cubic/lamellar composite material (6 days) exhibits a clear mesopore filling step and in addition also has an unusual hysteresis at medium to high partial pressure.[25] The composite cubic/lamellar sample exhibits significantly high surface area (757 m^2/g) and pore volume (0.78 cm^3/g). Isotherm d (Figure 3) is consistent with the existence of a composite material that consists of well-ordered cubic MCM-48 and lamellar material for the sample synthesized for 6 days. The sharp mesopore-filling step can be attributed to the MCM-48 phase while the unusual hysteresis is contributed by the lamellar component. (The XRD pattern of this material, after calcination, gives the impression of well-ordered MCM-48 simply because the lamellar component of the composite material collapses and is not "visible" in the XRD pattern). The isotherm of the calcined pure lamellar material (12 days) shows no clear evidence of a narrow pore size distribution and is dominated by the hysteresis at medium to high partial pressure. The hysteresis is characterized by a sharp step in the desorption isotherm. The sharp step has previously been ascribed to delayed capillary evaporation from (meso)pores with narrow constrictions.[25,27]

It is noteworthy that the calcined molecularly ordered lamellar sample has a relatively high surface area (637 m^2/g) and pore volume (0.68 cm^3/g). The pore volume is particularly high compared to that previously reported for comparable materials.[25] In addition, *t*-plot analysis revealed that the molecularly ordered lamellar sample had a micropore volume of 0.05 cm^3/g (i.e., only 7% of total pore volume) consistent with its mesoporous character. It is worthwhile to note that the hysteresis observed for the sorption isotherms of the cubic/lamellar composite and pure phase lamellar samples may also suggest the presence of aggregates made up of platy particles.[28] Furthermore, the observed hysteresis loop is typical of slit-shaped pores or spaces between parallel plates.[28] Such hysteresis is usually observed for porous layered materials such as pillared clays.[29] Indeed, the sorption isotherm of the calcined lamellar material (12 days) is very similar to isotherms normally observed for pillared clays.[29] This is perhaps an indication that, on calcination, the molecularly ordered lamellar silicate−surfactant mesophase is transformed into a (meso)porous pillared clay-type layered silica material. The high surface area and pore volume observed for this material is consistent with this suggestion.

Representative scanning electron microscopy (SEM) micrographs obtained for the various samples are shown in Figure 4. The hexagonal phase (MCM-41) sample (3 h) is mainly made up of submicrometer-sized free-standing or aggregated sphere-shaped particles. Larger rodlike particles are also observed. Such rodlike particles are not unusual for MCM-41 materials prepared under hydrothermal conditions.[17,30] On extending the crystal-

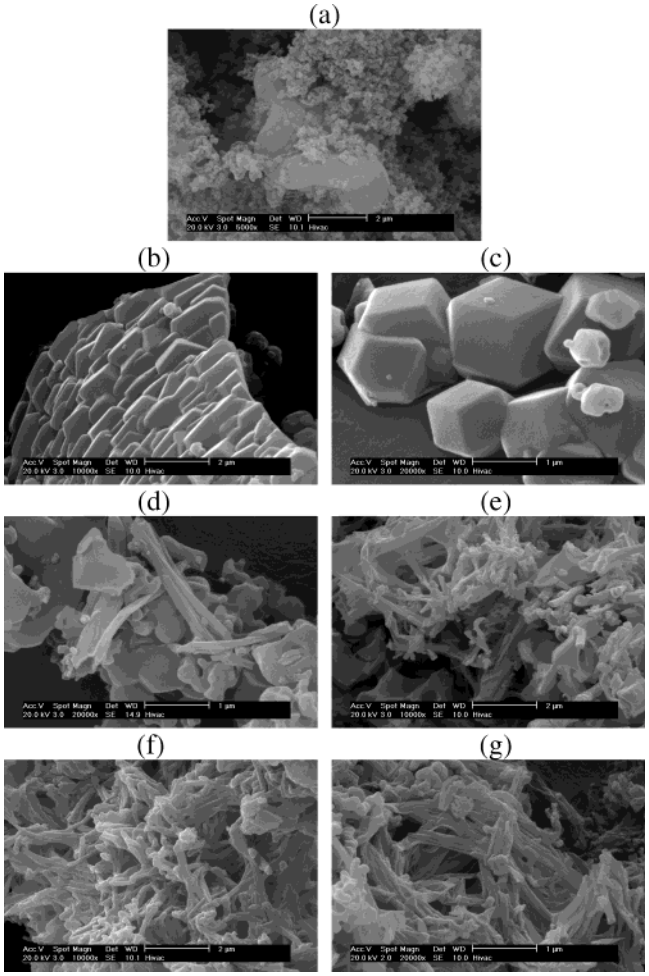

Figure 4. Representative SEM images for the various mesoporous silicas: (a) 3 h, hexagonal phase MCM-41; (b,c) 1 day, cubic phase MCM-48; (d) 4 days, cubic phase MCM-48; (e) 6 days, cubic/lamellar composite material and molecularly ordered lamellar silicate−surfactant mesophase before (f) and after (g) calcination.

lization time to 1 day, the spherical MCM-41 particles are transformed into the cubic phase (MCM-48) made up of well-formed cubic (rhombic dodecahedral) crystals.[23,24,31] In some cases, the crystals overlap, appearing to grow into one another as shown in Figure 4b. After 4 days of crystallization, the well-formed cubic MCM-48 crystals start to undergo a transformation into flaky elongated particles as shown in Figure 4d. The cubic (i.e., rhombic dodecahedral) MCM-48 crystals are no longer observed after 6 days of crystallization (Figure 4e); the particle morphology is transformed into mainly interconnected flaky particles. After 12 days of crystallization, only the aggregated/interconnected flaky threadlike particles are observed. The flaky threadlike particles are therefore a characteristic of the lamellar phase. The particle morphology of the lamellar phase obtained after 12 days of crystallization does not change after calcination, as shown by the comparison of the morphology before (Figure 4f) and after (Figure 4g) calcination.

The overall picture that emerges from the XRD, SEM, and nitrogen sorption studies is that increasing the time allowed for crystallization causes transformation of an initially hexagonal mesoporous silica phase onto a cubic phase. The hexagonal−cubic transformation occurs within 24 h of crystallization. The cubic phase is then maintained for crystallization periods of up to 100 h. After 6 days (144 h) of crystallization, the cubic phase slowly transforms to a lamellar phase, which exhibits local molecular ordering. After 12 days of crystallization, the cubic−lamellar transformation is complete and a molecularly ordered layered silicate−surfactant mesophase is obtained. The molecular ordering is only observed when the lamellar phase is present. It is therefore likely that the formation of a molecularly ordered silica network, at long crystallization time, acts as a driving force for the cubic−lamellar transformation.

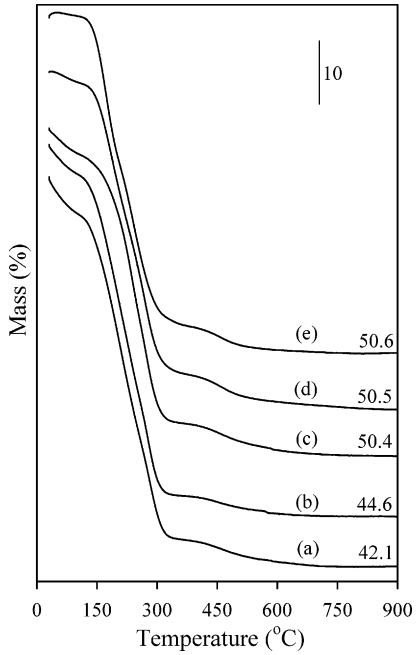

Figure 5. Thermogravimetric analysis curves of as-synthesized silicate−surfactant mesophases obtained from the hydrothermal crystallization of synthesis gels (of molar composition 1:0.28:42 SiO_2:CTAOH:H_2O) at 135 °C for (a) 3 h, (b) 1 day, (c) 4 days, (d) 6 days, and (e) 12 days. The values on the curves are the residual weight (%) at 800 °C.

3.2. Thermogravimetric Analysis of the Various Silica Phases. Thermogravimetric analysis curves obtained for the various as-synthesized silicate−surfactant mesophases are shown in Figure 5. In all cases the surfactant was desorbed in two steps.[25] However, the desorption maximas varied from sample to sample. The MCM-41 (3 h) and MCM-48 (1 and 4 days) samples had two weight loss events at ca. 207 and 285 °C. The cubic/lamellar composite sample had weight losses centered at 190 and 270 °C. The weight loss events from the molecularly ordered lamellar surfactant−silicate mesophase were at lower temperatures; 170 and 245 °C. This shift to lower surfactant "burn off" temperatures for the lamellar material has previously been reported by Kruk et al.[25,32] and is further evidence that the molecularly ordered mesophase obtained after 12 days of crystallization is purely lamellar. However, in contrast to previous reports,[25] we observed a lower CTA/SiO_2 ratio for the lamellar sample (0.189) compared to that for the cubic (0.226) and hexagonal (0.238) materials. The lower CTA/SiO_2 ratio observed here for the lamellar sample may be related to the fact that the framework is molecularly ordered. In general, the CTA/SiO_2 ratio decreased with increase in crystallization time and was in all cases lower than the synthesis gel (CTAB/SiO_2) ratio of 0.28. It is therefore likely that the high-to-low curvature phase transitions observed here proceeded via reconstruction of the silicate framework but without complete dissolution of the existing silica network during transformations.[18] Furthermore, since no significant changes in the pH of the synthesis gels were observed with increase in crystallization time, it is reasonable to conclude that the phase transformations occurred in an epitaxial manner.

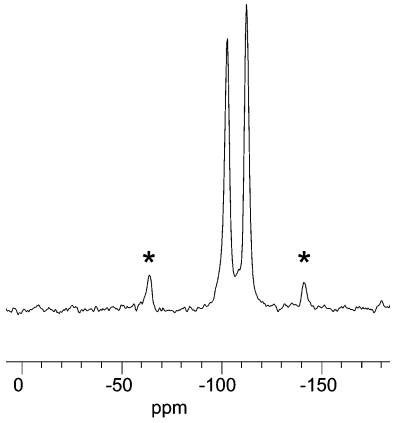

Figure 6. ^{29}Si CP/MAS NMR of molecularly ordered layered silicate−surfactant mesophase obtained after hydrothermal synthesis for 12 days. (* Denotes spinning sideband).

3.3. Si MAS NMR of Layered Silica Phase. To confirm that the lamellar material obtained after 12 days of crystallization contained some nanoscale or molecularly ordered, we performed ^{29}Si CP/MAS NMR.[15,16] The ^{29}Si CP/MAS NMR spectrum, shown in Figure 6, exhibits two well-resolved and narrow (fwhm ~2.5 ppm) resonances at −102 ppm (Q^3) and −112 ppm (Q^4). The resonances are due to silicons in $Si(OSi)_3OH$ (Q^3) or $Si(OSi)_4$ (Q^4) environments. The absence of a Q^2 ($Si(OSi)_2OH$) Si peak at ca. − 90 ppm indicates a relatively high level of silica condensation within the framework. This is consistent with the low CTA/SiO_2 ratio discussed above and may be related to (framework) crystallization-induced densification of the lamellar silica network.[22,33] The ^{29}Si CP/MAS NMR spectrum (Figure 6) is very similar to that previously reported for directly prepared molecularly ordered lamellar surfactant−silicate composites[16] and differs significantly from the spectra normally observed for conventional mesoporous silicas (Figure 2 in the Supporting Information shows a typical as-synthesized mesoporous silica sample).

3.4. Structural Ordering of Layered Silica Phase. We used transmission electron microscopy (TEM) to further probe the structural (pore) ordering of the molecularly ordered lamellar material before and after calcination. This is important because lamellar silicate−surfactant mesophases are considered to be unstable to calcination whereby they lose any structural ordering.[1,2] We note that a representative TEM micrograph (and corresponding selected area electron diffraction, SAED, pattern) of the as-synthesised lamellar silicate−surfactant mesophase (Figure 3 in the Supporting Information) show evidence of structural pore ordering (TEM) and ordering within the pore walls (SAED). (We note that it was difficult to obtain TEM images of the as-synthesized samples due to their instability under an electron beam). However, it was possible to observe pore channels that run along the particle axis. The SAED pattern shows diffuse diffraction rings, which is an indication that the lamellar material exhibits some local nanoscale or molecular ordering.[17] The SAED is therefore consistent with the XRD patterns and ^{29}Si CP/MAS NMR spectrum of the lamellar material.

More interesting is the observation that, after calcination, the lamellar mesoporous silica still exhibits structurally well-ordered domains as shown in Figure 7. The TEM micrographs (Figure 7) of the calcined template-free lamellar silica show particles with ordered pore arrangements. The particle shape is consistent with the flaky particle morphology (shown in Figure 4g) of the calcined lamellar silica. The existence of pore ordering is also consistent with the relatively high surface area and pore volume

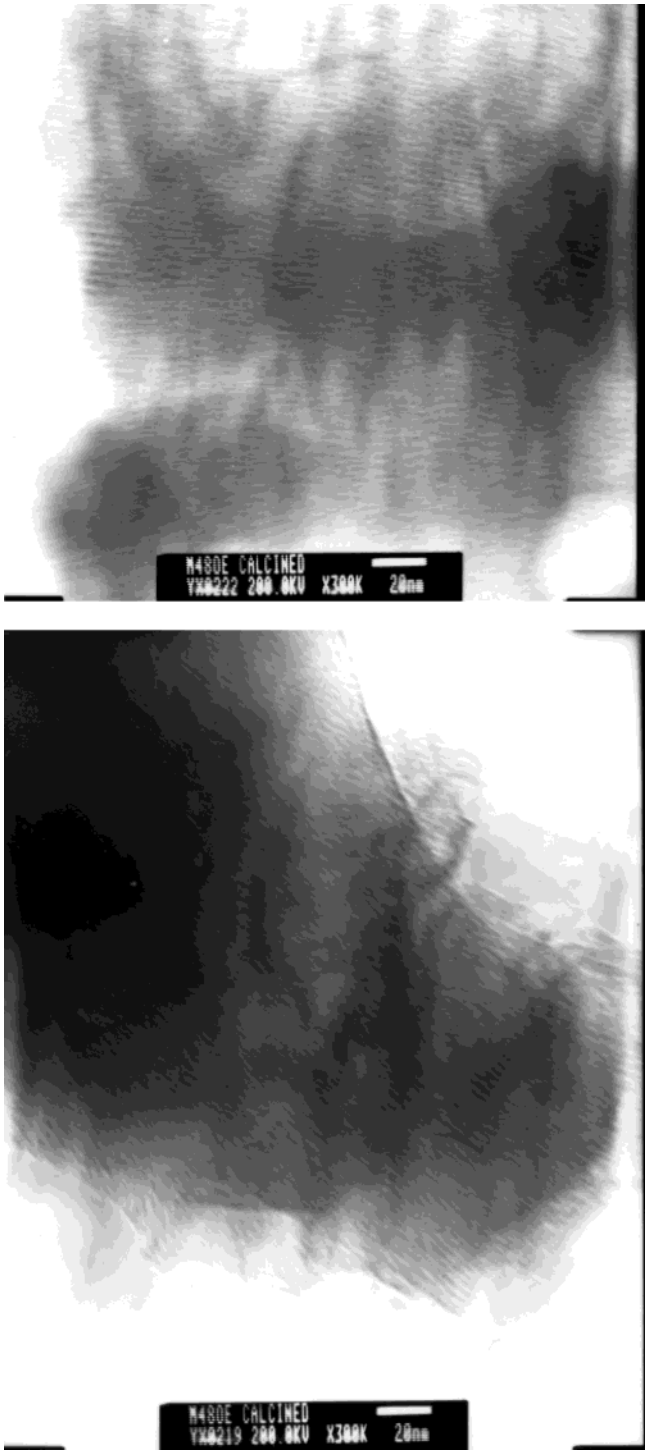

Figure 7. Representative TEM micrographs for the calcined molecularly ordered layered silica phase obtained after 12 days of synthesis. The micrographs show that the materials are structurally well-ordered.

observed for the calcined lamellar silica (Table 1). It is therefore likely that the layered silica is, to some extent, stable to calcination and template removal. We speculate that the calcined lamellar mesoporous silica may be stabilized by pillar-type structures formed from touching (due to thickness undulation or bending) of layers.[34] We have considered the possibility that the structurally ordered domains are from contamination with cubic or hexagonal phases; this is however unlikely since all the evidence (powder XRD, SEM, and nitrogen sorption studies) shows that the material obtained after 12 days of crystallization is a pure lamellar phase. To the best of our knowledge, this is

the first time that apparently stable layered mesoporous silica whose mesophase exhibits some evidence (from powder XRD, NMR, and SAED) of nanoscale or molecular ordering within the silica network has been prepared via a surfactant-mediated synthesis route.

4. Conclusions

We have described phase transformations from hexagonal (MCM-41) to cubic (MCM-48) and finally to a molecularly ordered layered silicate−surfactant mesophase achieved by simply changing the time allowed for hydrothermal crystallization of simple $CTAOH/SiO_2/H_2O$ systems at 135 °C. This is a departure from previous reports where molecularly ordered lamellar silicate−surfactant composites were prepared directly. The high-to-low curvature phase transitions appear to proceed via reconstruction of the silicate framework, in an epitaxial manner, without complete dissolution of the existing silica network during transformations. The transformation from the cubic to layered phase is accompanied by the emergence of molecular ordering in the silica framework. The molecular ordering is only observed when the lamellar phase is present. It is therefore likely that the formation of a molecularly ordered silica network, at long crystallization time, acts as a driving force for the cubic−lamellar phase transformation. The molecular ordering of the layered phase was confirmed using powder X-ray diffraction and (silicon-29) solid-state NMR. Changes in particle morphology and a gradual densification and increase in condensation of the silica network accompanied the phase transformations. We have, for the first time, characterized calcined lamellar mesoporous silica and show that it is possible to obtain a (meso)porous material (with high surface area and pore volume) which, to some extent, retains some framework molecular ordering and structurally well-ordered domains even after template removal by calcination. On a more general note, our findings provide some new insights on the mechanisms via which the formation of molecularly ordered mesoporous silica mesophases occur. Our findings therefore have important implications on the development of mesostructured silica-based materials that are porous and truly crystalline.

Acknowledgment. We thank the EPSRC for financial support.

Supporting Information Available: Additional supporting figures. This material is available free of charge via the Internet at http://pubs.acs.org.

References and Notes

(1) Kresge, C. T.; Leonowicz, M. E.; Roth, W. J.; Vartuli, J. C.; Beck, J. S. *Nature* **1992**, *359*, 710. (b) Beck, J. S.; Vartuli, J. C.; Roth, W. J.; Leonowicz, M. E.; Kresge, C. T.; Schmitt, K. D.; Chu, C. T.-W.; Olson, D. H.; Sheppard, E. W.; McCullen, S. B.; Higgins, J. B.; Schlenker, J. L. *J. Am. Chem. Soc.* **1992**, *114*, 10834.

(2) Ying, J. Y.; Mehnert, C. P.; Wong, M. S. *Angew. Chem., Int. Ed.* **1999**, *38*, 56. (b) Øye, G.; Sjöblom, J.; Stöcker, M. *Adv. Colloid Interface Sci.* **2001**, *89*, 439. (c) On, D. T.; Desplantier-Giscard, D.; Danumah, C.; Kaliaguine, S. *Appl. Catal., A* **2002**, *222*, 299.

(3) Guo, W. P.; Huang, L. M.; Deng, P.; Xue, Z. Y.; Li, Q. Z. *Microporous Mesoporous Mater.* **2001**, *44*−*45*, 427.

(4) (a) Guo, W. P.; Xiong, C. R.; Huang, L. M.; Li, Q. Z. *J. Mater. Chem.* **2001**, *11*, 1886. (b) Xia, Y.; Mokaya, R. *J. Mater. Chem.* **2004**, *14*, 863.

(5) Poladi, R. H. P. R.; Landry, C. C. *J. Solid State Chem.* **2002**, *167*, 363.

(6) Karlsson, A.; Stöcker. M.; Schmidt, R. *Microporous Mesoporous Mater.* **1999**, *27*, 181.

(7) Goto, Y.; Fukushima, Y.; Ratu, P.; Imada, Y.; Kubota, Y.; Sugi, Y.; Ogura, M.; Matsukata, M. *J. Porous Mater.* **2002**, *9*, 43.

(8) Kloetstra, K. R.; van Bekkum, H.; Jansen, J. C. *Chem. Commun.* **1997**, 2281.

(9) Huang, L.; Guo, W.; Deng, P.; Xue, Z.; Li, Q. *J. Phys. Chem. B* **2000**, *104*, 2817.

(10) On, D. T.; Kaliaguine, S. *Angew. Chem., Int. Ed.* **2001**, *40*, 3248.

(11) On, D. T.; Kaliaguine, S. *Angew. Chem., Int. Ed.* **2002**, *41*, 1036.

(12) Liu, Y.; Zhang, W.; Pinnavaia, T. J. *J. Am. Chem. Soc.* **2000**, *122*, 8791.

(13) Liu, Y.; Zhang, W.; Pinnavaia, T. J. *Angew. Chem., Int. Ed.* **2001**, *40*, 1255.

(14) Zhang, Z.; Han, Y.; Zhu, L.; Wang, R.; Yu, Y.; Qiu, S.; Zhao, D.; Xiao, F.-S. *Angew. Chem., Int. Ed.* **2001**, *40*, 1258. (b) Zhang, Z.; Han, Y.; Xiao, F.-S.; Qiu, S.; Zhu, L.; Wang, R.; Yu, Y.; Zou, B.; Wang, Y.; Sun, H.; Zhao, D.; Wei, Y. *J. Am. Chem. Soc.* **2001**, *123*, 5014. (c) Liu, J.; Zhang, X.; Han, Y.; Xiao, F. S. *Chem. Mater.* **2002**, *14*, 2536.

(15) Christiansen, S. C.; Zhao, D. Y.; Janicke, M. T.; Landry, C. C.; Stucky, G. D.; Chmelka, B. F. *J. Am. Chem. Soc.* **2001**, *123*, 4519.

(16) Wang, L. Q.; Exarhos, G. J. *J. Phys. Chem. B* **2003**, *107*, 443.

(17) Mokaya, R. *Chem. Commun.* **2001**, 1092.

(18) Landry, C. C.; Tolbert, S. H.; Gallis, K. W.; Monnier, A.; Stucky, G. D.; Norby, P.; Hanson, J. C. *Chem. Mater.* **2001**, *13*, 1600.

(19) Tolbert, S. H.; Landry, C. C.; Stucky, G. D.; Chmelka, B. F.; Norby, P.; Hanson, J. C.; Monnier, A. *Chem. Mater.* **2001**, *13*, 2247.

(20) Gross, A. F.; Le, V. H.; Kirsch, B. L.; Riley, A. E.; Tolbert, S. H. *Chem. Mater.* **2001**, *13*, 3571.

(21) Romero, A. A.; Alba, M. D.; Zhou, W.; Klinowski, J. *J. Phys. Chem. B* **1997**, *101*, 5294.

(22) Xu, J.; Luan, Z. H.; He, H. Y.; Zhou, W.; Kevan, L. *Chem. Mater.* **1998**, *10*, 3690.

(23) Xia, Y.; Mokaya, R. *J. Mater. Chem.* **2003**, *13*, 657.

(24) Sayari, A. *J. Am. Chem. Soc.* **2000**, *122*, 6504. (b) Kruk, M.; Jaroniec, M.; Ryoo, R.; Kim, J. M. *Chem. Mater.* **1999**, *11*, 2568.

(25) Kruk, M.; Jaroniec, M.; Pena, M. L.; Rey, F. *Chem. Mater.* **2002**, *14*, 4434.

(26) Hou, Q.; Margolese, D.; Stucky, G. D. *Chem. Mater.* **1996**, *8*, 1147.

(27) Kruk, M.; Jaroniec, M. *Chem. Mater.* **2001**, *13*, 3169.

(28) Gregg, S. J.; Sing, K. S. W. *Adsorption, Surface Analysis and Porosity*; Academic Press: London, 1982. (b) Sing, K. S. W.; Everett, D. H.; Haul, R. A. W.; Moscou, L.; Pierotti, R. A.; Rouquerol, J.; Siemieniewska, T. *Pure Appl. Chem.* **1985**, *57*, 603.

(29) Pinnavaia, T. J. *Science* **1983**, *220*, 365. (b) Gil, A.; Gandia, L. M.; Vicente, M. A. *Catal. Rev.-Sci. Eng.* **2000**, *42*, 145. (c) Ding, Z.; Kloprogge, J. T.; Frost, R. L.; Lu, G. Q.; Zhu, H. *J. Porous Mater.* **2001**, *8*, 273. (d) Jones, W. *Catal. Today* **1988**, *2*, 357.

(30) Mokaya, R.; Zhou, W.; Jones, W. *J. Mater. Chem.* **2000**, *10*, 1139. (b) Mokaya, R. *Microporous Mesoporous Mater.* **2001**, *44*−*45*, 119. Xia, Y.; Mokaya, R. *J. Mater. Chem.* **2003**, *13*, 3112.

(31) Kim, J. M.; Kim, S. K.; Ryoo, R. *Chem. Commun.* **1998**, 259. (b) Kaneda, M.; Tsubakiyama, T.; Carlsson, A.; Sakamoto, Y.; Ohsuna, T.; Terasaki, O.; Joo, S. H.; Ryoo, R. *J. Phys. Chem. B* **2002**, *106*, 1256.

(32) Kruk, M.; Jaroniec, M.; Yang, Y.; Sayari, A. *J. Phys. Chem. B* **2000**, *104*, 1581.

(33) Fyfe, C. A.; Fu, G. *J. Am. Chem. Soc.* **1995**, *117*, 9709.

(34) Zhou, Y.; Antonietti, M. *Adv. Mater.* **2003**, *15*, 1452.